UC Riverside
UC Riverside Previously Published Works

Title

Layer-dependence study of two-dimensional ferromagnets: Fe3GeTe2 and Fe5Ge2Te2

Authors

Alghamdi, Mohammed

Jothi, Palani R

Liao, Wei-Cheng

et al.

Peer reviewed

Layer-dependence study of two-dimensional ferromagnets: Fe_3GeTe_2 and $Fe_5Ge_2Te_2$ FREE

Mohammed Alghamdi ; Palani R. Jothi ; Wei-Cheng Liao ; Sinisa Coh ; Xianqing Lin ;
Boniface P. T. Fokwa ; Jing Shi

Check for updates

View Online

Export Citation

Layer-dependence study of two-dimensional ferromagnets: Fe_3GeTe_2 and $Fe_5Ge_2Te_2$

Mohammed Alghamdi,[1] (iD) Palani R. Jothi,[2] (iD) Wei-Cheng Liao,[1] (iD) Sinisa Coh,[3] (iD) Xianqing Lin,[4] (iD)
Boniface P. T. Fokwa,[2] (iD) and Jing Shi[1,a)] (iD)

AFFILIATIONS

[1]Department of Physics and Astronomy, University of California, Riverside, California 92521, USA
[2]Department of Chemistry, University of California, Riverside, California 92521, USA
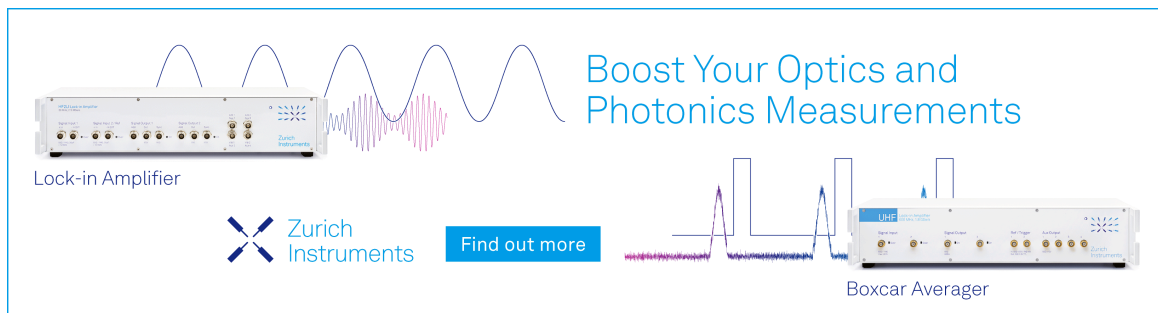[3]Materials Science and Engineering and Mechanical Engineering Department, University of California, California 92521, USA
[4]College of Science, Zhejiang University of Technology, Hangzhou 310023, China

[a)]Author to whom correspondence should be addressed: jing.shi@ucr.edu

ABSTRACT

We have investigated the electrical transport properties of nanodevices fabricated from exfoliated flakes of two-dimensional metallic ferromagnets Fe_3GeTe_2 (FGT) and $Fe_5Ge_2Te_2$ (FG2T) down to below three layers in thickness. The per-layer anomalous Hall conductivity even in thick FGT and FG2T devices is found to be much smaller than $\sim\frac{e^2}{h}$, the approximate value calculated for thick undoped crystals. Moreover, we obtain a power-law scaling relation between the per-layer anomalous Hall and per-layer longitudinal conductivities with an exponent close to 1.6, which agrees with the universal value for poor ferromagnetic conductors. Both FGT and FG2T devices show clear layer-dependent Curie temperatures and layer-dependent perpendicular magnetic anisotropy, with FG2T dominating the former and FGT dominating the latter for all thicknesses. Despite their declining trend as the device thickness decreases, both Curie temperature and magnetic anisotropy retain a significant fraction of their bulk values (>60% and >80% of the bulk values, respectively, even in the thinnest FG2T device), indicating attractive potential for practical applications.

Published under an exclusive license by AIP Publishing. https://doi.org/10.1063/5.0207209

The discoveries of remarkable properties of two-dimensional (2D) magnets including $Cr_2Ge_2Te_6$ (CGT),[1] CrI_3,[2] Fe_3GeTe_2 (FGT),[3–5] and $MnBi_2Te_4$[6] have generated immense research interest in the communities of 2D materials and low-dimensional magnetism.[7,8] Apart from many intriguing layer-dependent phenomena inherent to single 2D materials, heterostructures containing these materials offer essentially unlimited opportunities to explore novel effects such as spin–orbit torques,[9–11] spin textures,[12,13] magnetic tunnel junctions,[14] exchange bias,[15] and proximity-induced ferromagnetism.[16–18] Among 2D ferromagnets, FGT stands out as an excellent prototype because of its metallicity, unusually strong perpendicular magnetic anisotropy (PMA), predicted strong magnetostriction effect,[19] high and widely tunable Curie temperature (T_C),[5,20–22] etc. FGT is recently joined by other members in this class of 2D ferromagnets such as $Fe_5Ge_2Te_2$ (FG2T)[23] and Fe_3GaTe_2,[24] which show higher even above room-temperature T_C in addition to other similar attributes such as lattice structure and strong PMA. In this comparative study of FGT and FG2T, we focus on the anomalous Hall effect (AHE), T_C, and magnetic anisotropy in nanodevices fabricated from FGT and FG2T down to below three layers.

Three-dimensional (3D) FGT and FG2T unit cells are shown in Fig. 1(a). Both FGT and FG2T bulk crystals are grown by the solid-state reaction method, structurally and magnetically characterized as previously reported.[9,23] The fabrication of FGT and FG2T nanodevices starts with the exfoliation of flakes with thicknesses ranging from 100 layers down to below three layers. The thickness of devices with three or more layers can be more precisely determined from the atomic force microscopy. For the thinnest FG2T device, the exact thickness is certain, but it is clearly below 3L as judged by optical microscopy, resistivity, and AHE magnitude. Experimental determination of the flake thickness is described in the supplementary material. To protect nanodevices, one of the two methods is adopted to prevent oxidation (see S1 of the supplementary material). Figure 1(b) displays optical images of two representative devices fabricated with both methods. We note that the electrical transport properties of both types of nanodevices remain unchanged over months, indicating excellent stability. All devices show linear current–voltage characteristics indicative of Ohmic contact. Longitudinal resistivity and Hall effect measurements are performed in either Quantum Design's Physical Property Measurement

(A)

(B)

(C)
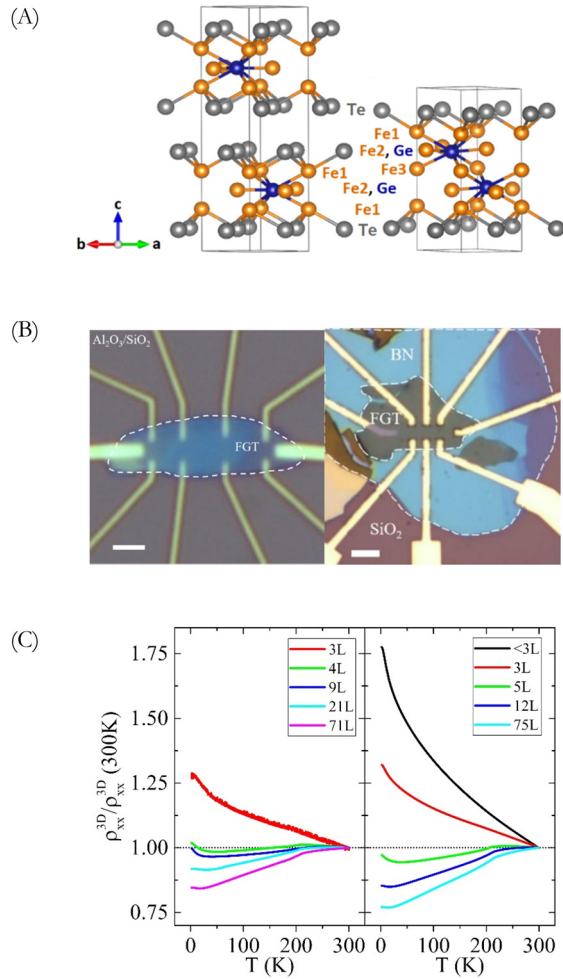
FIG. 1. (a) Unit cells of FGT and FG2T. FGT consists of two layers with a total thickness of 1.6 nm, while FG2T has a single layer with a thickness of 1.08 nm. (b) Left image is a 9L FGT device protected with 20 nm Al_2O_3. The dashed white line shows the boundary of 9L FGT flake on SiO_2, and the scale bar is 2 μm. Right image is a BN-covered FGT device. The white dashed lines show the contours of FGT and BN flakes on SiO_2. The scale bar is 3 μm. (c) Longitudinal resistivity of FGT (left) and FG2T (right) as a function of temperature for devices with various thicknesses.

System (PPMS) or a closed-cycle refrigerator down to low temperatures (2 and 4 K, respectively). The PMA field is extracted from the saturation of the Hall signals with the magnetic field applied parallel to atomic layers using PPMS.

The normalized resistivity of FGT and FG2T nanodevices fabricated with Method 1 is plotted in Fig. 1(c). The thickness ranges from 70+ layers down to below 3L (for FG2T). The mean value of the room-temperature resistivity is ~350 $\mu\Omega$ cm (see S2 of the supplementary material), 1–2 orders of magnitude more resistive than typical ferromagnetic metals. In thicker devices, the resistivity is metallic, i.e., decreasing resistivity with decreasing temperature. The average rate of resistivity decrease over the entire temperature range is ~25% from the room-temperature values in 75L FG2T devices and becomes smaller in thinner devices. Below 5L, however, the resistivity starts to

show an insulating behavior, i.e., increasing resistivity as the temperature is decreased. Similar insulating behavior for thin FGT devices was previously observed by other researchers.[3,5] Since the resistivity of thin devices is more sensitive to surface oxidation, one suspicion is that the surface properties may have been somewhat altered due to the brief air exposure with method 1. To examine this possibility, we fabricated thin FGT devices using method 2 and measured their transport properties. The insulating behavior is reproduced in a 3L device (see Fig. S6 in the supplementary material); therefore, we exclude the oxidation effect as the cause of the insulating behavior. While the underlying mechanisms differ (e.g., weak localization, Kondo effect, and hopping), some 3D magnetic thin films (e.g., manganites[25,26] and $NdTiO_3$[27]) also exhibit a low-temperature insulating trend in the thin limit.

Figures 2(a) shows the Hall resistivity results in 3L FGT and 3L FG2T devices for selected temperatures down to 2 K. From more detailed analysis (see S5 of the supplementary material), we find that T_C is ~192 and ~193 K for FGT and FG2T, respectively. Both devices show rather squared hysteresis loops at low temperatures. It is clear that the total R_{yx} signals are dominated by AHE, i.e., the second term in $R_{yx} = R_0H + R_SM$ that is proportional to the magnetization M; hence, we equate the total Hall signal approximately to the AHE signal by ignoring the ordinary Hall effect represented by the first term. From the slope of the ordinary Hall responses measured at room temperature, we find that the carrier concentration is ~ 2×10^{21}/cm^3, which gives a mobility value of ~10 cm^2/V s. We plot the magnitude of the AHE resistivity scaled by the 2 K value as a function of temperature T in Fig. 2(b) for a few representative FGT (left) and FG2T (right) devices. It is interesting that the thin devices show a smaller curvature than the thick ones, which resemble the mean-field-like T-dependence of M. Meanwhile, we also know that because of the power-law scaling relation $R_S \propto R_{xx}^n$, additional T-dependence of R_{xx} shown in Fig. 1(c) can skew the shape of the mean-field-like M vs T curve in R_{yx}. In particular, the concave curvature of the insulating-like R_{xx} in 3L devices makes the R_{yx} vs T curves in Fig. 2(b) appear to be almost linear.

From the measured R_{yx} and the sheet resistance at 2 K, we calculate the 2D anomalous Hall conductance G_{xy}. Figure 3(a) shows G_{xy} vs the number of layers N for all devices. Clearly, G_{xy} is approximately proportional to N, but with large error bars for some devices which come from the uncertainty in determining the effective aspect ratio for calculating the sheet resistance. A similar linear relationship is found for the longitudinal conductance vs N (not shown here). From those data, we calculate the per-layer anomalous Hall conductivity (AHC) σ_{xy}^L and per-layer longitudinal conductivity σ_{xx}^L and plot the data in Fig. 3(b). Despite the uncertainties in both quantities (see S3 of the supplementary material), the plot reveals the following interesting information. First, the σ_{xy}^L values of FGT and FG2T devices fall in the same range and do not show any distinguishable difference. Second, σ_{xy}^L varies by a factor of ~10, but the largest value is ~0.15 $\frac{e^2}{h}$, still much smaller than ~$\frac{e^2}{h}$, the predicted value for intrinsic contribution to σ_{xy}^L based on the Berry curvature calculations for thick undoped FGT[28] and FG2T.[29] While the actual samples may be slightly off stoichiometry, the results from the nominally undoped FGT and FG2T in this work are apparently inconsistent with the intrinsic origin of the AHE in FGT and FG2T. Third, within experimental uncertainty, there appears to be a linear correlation between σ_{xx}^L and σ_{xy}^L on this log–log plot, which means a power-law relation between the two quantities. The previously mentioned scaling relation $R_S \propto R_{xx}^n$ is equivalent to
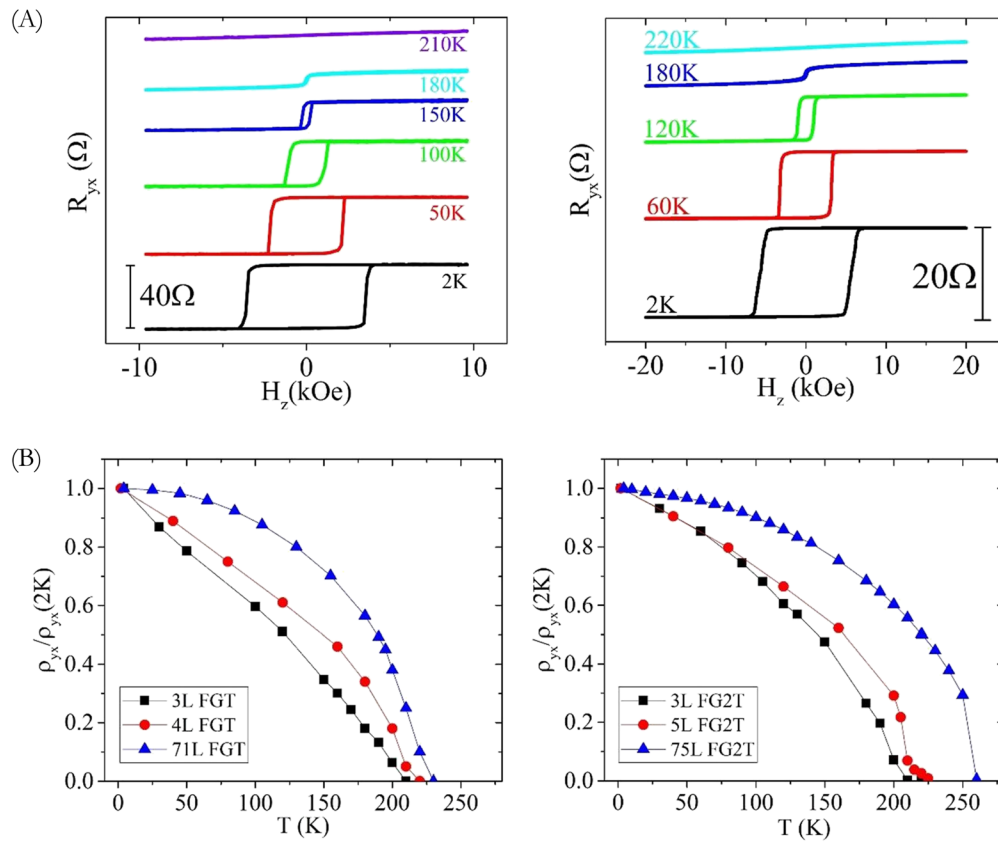
FIG. 2. Anomalous Hall loops for 3L devices for both FGT (left) and FG2T (right) at selected temperatures. (b) Temperature dependence of scaled anomalous Hall resistivity magnitude of three representative devices for FGT (left) and FG2T (right).

$\sigma_{xy}^L \propto (\sigma_{xx}^L)^{2-n}$. We obtain the exponent 2-n from the linear fits to the data in Fig. 3(b), which is found to vary from 1.4 to 1.9 (i.e., n from 0.1 to 0.6). Decades of the AHE studies[30] have established that the intrinsic AHE is scattering-rate independent, which gives rise to n = 2, while for skew scattering, n = 1. The former yields a constant σ_{xy}^L as the resistivity or conductivity varies, but the latter leads to a linear relation, $\sigma_{xy}^L \sim \sigma_{xx}^L$. The exponent obtained from our experimental data in Fig. 3(b) further refutes the intrinsic mechanism since σ_{xy}^L clearly has σ_{xx}^L-dependence. In addition, it is well known that skew scattering becomes dominant only in the clean limit,[30] i.e., the regime with high conductivity. Our samples clearly do not fall in this regime either. We draw two reference lines on this plot, i.e., for 2-n = 1 (or n = 1) and 1.6 (or n = 0.4). Obviously, most data points are situated closer to the latter. Here, we stress that we do not have the ability to narrow the range of the exponent in our fitting due to scattered experimental data. We note that a different exponent for a FGT device was previously reported in the literature.[31]

In poorly conducting ferromagnetic materials showing hopping conductivity with $\sigma_{xx} < 10^4 \, \Omega^{-1} \, \text{cm}^{-1}$, a universal scaling relation, $\sigma_{xy} \propto \sigma_{xx}^{1.6}$, was observed in many studies.[32] Our data are better described by this scaling relation. Recall that even the room-temperature resistivity of both FGT and FG2T is two orders of magnitude l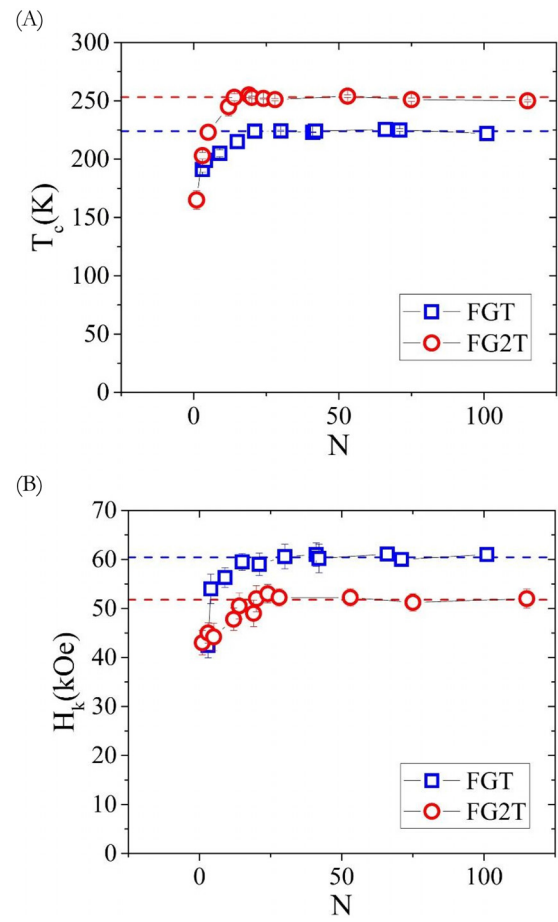arger than that of good metals. It puts FGT and FG2T in the poor conductor category. We note that a large effective mass of electrons in FGT was previously found from the specific heat measurements and interpreted by strong electron correlation.[33] The heavy electron mass can result in higher resistivity from the simple Drude model. Additionally, stronger correlation in thinner FGT may be present due to the confinement effect, which can lead to the observed insulating behavior.

In bulk FG2T crystals, incorporating more Fe-layers into the unit cell leads to a higher T_C than that of FGT. Here, we compare how T_C depends on the layer thickness in both materials. The layer-dependent T_C is determined from the AHE data (see S5 in the supplementary material). As shown in Fig. 4(a), at large thicknesses, i.e., $N > 20L$, T_C of both materials saturates at their bulk values, 225 and 255 K for FGT and FG2T, respectively, but below 20L, it shows a smooth declining trend. The greatly reduced T_C in ultrathin 3D ferromagnetic metals such as Ni and Co_1Ni_9 was interpreted as the finite size effect.[34] In these metal films, T_C was extrapolated zero at the monolayer limit. In contrast, in our thinnest FG2T device (monolayer or bilayer), T_C is still as high as ~160 K. For FGT, an estimated T_C value from extrapolation in Fig. 4(a) can be as high as 150 K at the monolayer limit, which is higher than previously reported values, e.g., ~125 and ~20 K in Refs. 4 and 5, respectively. In our FGT and FG2T devices, T_C at the monolayer limit is 60% larger than their respective bulk value.
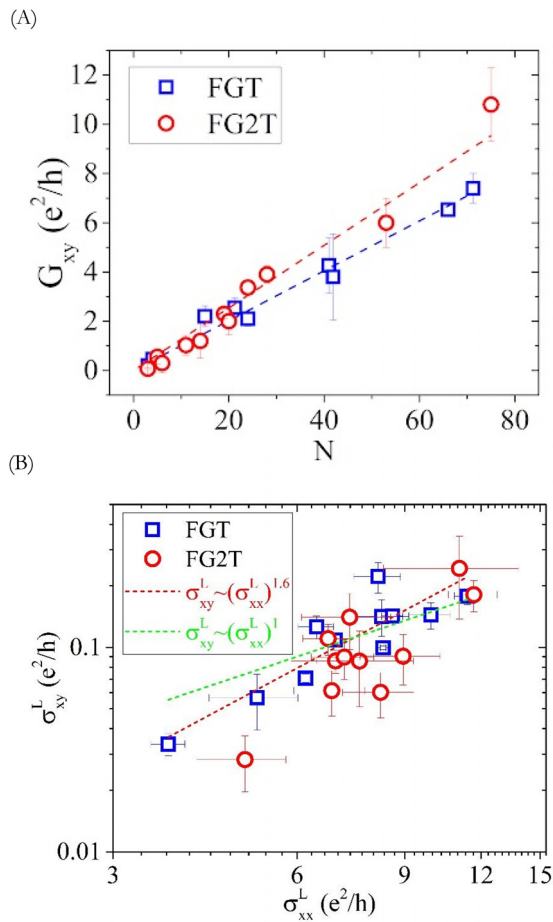
FIG. 3. (a) Layer number dependence of anomalous Hall conductance G_{xy} for both FGT and FG2T. (b) Per-layer anomalous Hall conductivity σ_{xy}^{L} vs per-layer longitudinal conductivity σ_{xx}^{L} on a log–log scale. Two straight lines are drawn for reference: the red for conductivity exponent (2-n) = 1.6 and the green for (2-n) = 1.

FIG. 4. (a) Layer number dependence of T_C of FGT and FG2T devices. (b) Layer number dependence of anisotropy field H_k of FGT and FG2T devices.

We perform the AHE measurements with the applied magnetic field oriented along the atomic layers that allow us to extract the anisotropy field, H_K, from the saturation behavior (see S6 of supplementary material), as a function of N as shown in Fig. 4(b), from which the magnetic anisotropy energy density K_1 can be calculated. Both FGT and FG2T thick devices have extraordinarily strong PMA, i.e., $K_1 \sim 10^7$ erg/cm^3 for FGT and $K_1 \sim 6 \times 10^6$ erg/cm^3 for FG2T at 2 K, which are much higher than many 3D ferromagnetic materials.[35] As shown in Fig. 4(b), H_K starts to decrease from their thick values when the layer number is below 12. Surprisingly, in the thinnest FG2T device, a very strong H_K ($\sim$43 kOe) is retained, which amounts to $\sim$81% of the bulk value. A similar H_K value is found for monolayer FGT from extrapolation, which is $\sim$70% of the bulk value. This remarkable property is highly desired for potential technological applications. Compared to FGT, the higher T_C in FG2T is somewhat expected due to closer Fe–Fe distance, which results in a stronger exchange interaction; however, the lower H_K in FG2T may not seem to be straightforward. Detailed density-functional theory (DFT) calculations confirm the experimental observation.[23] A qualitative argument

is that the anisotropy is strengthened through hybridization between Cr- and the neighboring Te-atoms via so-called off-site SOC just as in the study of $Cr_2Ge_2Te_6$ (CGT).[36] In FG2T, only the outer two Fe-layers are immediately adjacent to the Te-layers, leaving the other three Fe-layers farther away from the strong SOC source. In contrast, two out of three Fe-layers in FGT are adjacent to the Te-layers, leading to relatively stronger off-site SOC in FGT, and subsequently strong PMA. The resulting strong anisotropy magnifies the spin wave gap and, thus, suppresses the spin wave excitations; consequently, it stabilizes the ferromagnetism against thermal fluctuations even in the monolayer limit.

In summary, the observed smaller-than-predicted per-layer anomalous Hall conductivity in both FGT and FG2T follows the universal scaling relation for low-conductivity conductors, which does not favor either the intrinsic or skew scattering origin. In addition, the layer-dependent T_C and off-site SOC strengthened PMA show remarkably strong ferromagnetism down to the thinnest devices, which is highly desired for potential applications.

See the supplementary material for device fabrication details, experimental data on layer thickness dependence of longitudinal

resistivity, anisotropic magnetoresistance, Hall and longitudinal conductance calculations, Curie temperature determination, and anisotropy field determination.

AUTHOR DECLARATIONS
Conflict of Interest

The authors have no conflicts to disclose.

Author Contributions

Mohammed Alghamdi: Data curation (lead); Formal analysis (supporting); Investigation (lead); Writing – review & editing (equal). **Palani R. Jothi:** Investigation (supporting). **Wei-Cheng Liao:** Investigation (supporting). **Sinisa Coh:** Formal analysis (supporting); Writing – review & editing (equal). **Xianqing Lin:** Formal analysis (supporting). **Boniface P. T. Fokwa:** Investigation (supporting); Writing – review & editing (equal). **Jing Shi:** Conceptualization (equal); Funding acquisition (equal); Investigation (equal); Methodology (equal); Project administration (equal); Resources (equal); Supervision (equal); Validation (equal); Writing – original draft (equal); Writing – review & editing (equal).

DATA AVAILABILITY

The data that support the findings of this study are available within the article and its supplementary material.

REFERENCES

[1]C. Gong, L. Li, Z. Li, H. Ji, A. Stern, Y. Xia, T. Cao, W. Bao, C. Wang, Y. Wang, Z. Q. Qiu, R. J. Cava, S. G. Louie, J. Xia, and X. Zhang, "Discovery of intrinsic ferromagnetism in two-dimensional van der Waals crystals," Nature **546**, 265 (2017).

[2]B. Huang, G. Clark, E. Navarro-Moratalla *et al.*, "Layer-dependent ferromagnetism in a van der Waals crystal down to the monolayer limit," Nature **546**, 270 (2017).

[3]S. S. Liu, X. Yuan, Y. C. Zou *et al.*, "Wafer-scale two-dimensional ferromagnetic Fe_3GeTe_2 thin films grown by molecular beam epitaxy," npj 2D Mater. Appl. **1**, 30 (2017).

[4]Z. Y. Fei, B. Huang, P. Malinowski *et al.*, "Two-dimensional itinerant ferromagnetism in atomically thin Fe_3GeTe_2," Nat. Mater. **17**, 778 (2018).

[5]Y. Deng, Y. J. Yu, Y. Ch. Song *et al.*, "Gate-tunable room-temperature ferromagnetism in two-dimensional Fe_3GeTe_2," Nature **563**, 94 (2018).

[6]Y. J. Deng, Y. J. Deng, M. Z. Shi *et al.*, "Quantum anomalous Hall effect in intrinsic magnetic topological insulator $MnBi_2Te_4$," Science **367**, 895 (2020).

[7]K. S. Burch, D. Mandrus, and J.-G. Park, "Magnetism in two-dimensional van der Waals materials," Nature **563**, 47 (2018).

[8]M. Gibertini, K. Koperski, A. F. Morpurgo, and K. S. Novoselov, "Magnetic 2D materials and heterostructures," Nat. Nanotechnol. **14**, 408 (2019).

[9]M. Alghamdi, M. Lohmann, J. Li, P. R. Jothi, Q. Shao, M. Aldosary, T. Su, B. P. T. Fokwa, and J. Shi, "Highly efficient spin–orbit torque and switching of layered ferromagnet Fe_3GeTe_2," Nano Lett. **19**, 4400 (2019).

[10]V. Ostwal, T. T. Shen, and J. Appenzeller, "Efficient spin-orbit torque switching of the semiconducting van der Waals ferromagnet $Cr_2Ge_2Te_6$," Adv. Mater. **32**, 1906021 (2020).

[11]V. Gupta, T. M. Cham, G. M. Stiehl *et al.*, "Manipulation of the van der Waals magnet $Cr_2Ge_2Te_6$ by spin–orbit torques," Nano Lett. **20**, 7482 (2020).

[12]H. C. Xie, X. P. Luo, Z. P. Ye *et al.*, "Evidence of non-collinear spin texture in magnetic moiré superlattices," Nat. Phys. **19**, 1150 (2023).

[13]Y. Y. Wu, B. Francisco, Z. J. Chen *et al.*, "A van der Waals interface hosting two groups of magnetic skyrmions," Adv. Mater. **34**, 2110583 (2022).

[14]Z. Wang, D. Sapkota, T. Taniguchi, K. Watanabe, D. Mandrus, and A. F. Morpurgo, "Tunneling spin valves based on $Fe_3GeTe_2/hBN/Fe_3GeTe_2$ van der Waals heterostructures," Nano Lett. **18**, 4303 (2018).

[15]J.-Z. Fang, H.-N. Cui, S. Wang *et al.*, "Exchange bias in the van der Waals heterostructure $MnBi_2Te_4/Cr_2Ge_2Te_6$," Phys. Rev. B **107**, L041107 (2023).

[16]M. Lohmann, T. Su, B. Niu, Y. S. Hou, M. Alghamdi, M. Aldosary, W. Y. Xing, J. N. Zhong, S. Jia, W. Han, R. Q. Wu, Y. T. Cui, and J. Shi, "Probing magnetism in insulating $Cr_2Ge_2Te_6$ by induced anomalous Hall effect in Pt," Nano Lett. **19**, 2397 (2019).

[17]X. Yao, B. Gao, M.-G. Han *et al.*, "Record high-proximity-induced anomalous Hall effect in $(Bi_xSb_{1-x})_2Te_3$ thin film grown on $CrGeTe_3$ substrate," Nano Lett. **19**, 4567 (2019).

[18]J. X. Li, M. Rashetnia, M. Lohmann *et al.*, "Proximity-magnetized quantum spin Hall insulator: Monolayer 1T' $WTe_2/Cr_2Ge_2Te_6$," Nat. Commun. **13**, 5134 (2022).

[19]H. L. Zhuang, P. R. C. Kent, and R. G. Hennig, "Strong anisotropy and magnetostriction in the two-dimensional Stoner ferromagnet Fe_3GeTe_2," Phys. Rev. B **93**, 134407 (2016).

[20]Q. Li, M. M. Yang, C. Gong *et al.*, "Patterning-induced ferromagnetism of Fe_3GeTe_2 van der Waals materials beyond room temperature," Nano Lett. **18**, 5974 (2018).

[21]M. M. Yang, Q. Li, R. V. Chopdekar *et al.*, "Highly enhanced Curie temperature in Ga-implanted Fe_3GeTe_2 van der Waals material," Adv. Quantum Technol. **3**, 2000017 (2020).

[22]H. Y. Wang, Y. J. Liu, E. C. Wu *et al.*, "Above room-temperature ferromagnetism in wafer-scale two-dimensional van der Waals Fe_3GeTe_2 tailored by a topological insulator," Nano Lett. **14**, 10045 (2020).

[23]P. R. Jothi, Y. Zhang, J. P. Scheifers, M. Alghamdi, D. Stekovic, M. Itkis, J. Shi, and B. P. T. Fokwa, "$Fe_{5-x}Ge_2Te_2$—A new exfoliable itinerant ferromagnet with high Curie temperature and large perpendicular magnetic anisotropy," Phys. Status Solidi RRL **14**(3), 1900666 (2020).

[24]G. J. Zhang, F. Guo, H. Wu *et al.*, "Above-room-temperature strong intrinsic ferromagnetism in 2D van der Waals Fe_3GaTe_2 with large perpendicular magnetic anisotropy," Nat. Commun. **13**, 5067 (2022).

[25]W. Yuan, Y. L. Zhao, C. Tang *et al.*, "Epitaxial growth and properties of $La_{0.7}Sr_{0.3}MnO_3$ thin films with micrometer wide atomic terraces," Appl. Phys. Lett. **107**, 022404 (2015).

[26]W. Niu, M. Gao, X. F. Wang, F. Q. Song, J. Du, X. R. Wang, Y. B. Xu, and R. Zhang, "Evidence of weak localization in quantum interference effects observed in epitaxial $La_{0.7}Sr_{0.3}MnO_3$ ultrathin films," Sci. Rep. **6**, 26081 (2016).

[27]X. X. Cai, J. Yue, P. Xu, B. Jalan, and V. S. Pribiag, "From weak antilocalization to Kondo scattering in a magnetic complex oxide interface," Phys. Rev. B **103**, 115434 (2021).

[28]X. Q. Lin and J. Ni, "Layer-dependent intrinsic anomalous Hall effect in Fe_3GeTe_2," Phys. Rev. B **100**, 085403 (2019).

[29]X. Q. Lin, private communication (2023).

[30]N. Nagaosa, J. Sinova, S. Onoda, A. H. MacDonald, and N. P. Ong, "Anomalous Hall effect," Rev. Mod. Phys. **82**, 1539 (2010).

[31]J. S. Xu, W. A. Phelan, and C.-L. Chien, "Large anomalous Nernst effect in a van der Waals ferromagnet Fe_3GeTe_2," Nano Lett. **19**, 8250 (2019).

[32]T. Fukumura, H. Toyosaki, K. Ueno *et al.*, "A scaling relation of anomalous Hall effect in ferromagnetic semiconductors and metals," Jpn. J. Appl. Phys., Part II **46**, L642 (2007).

[33]J.-X. Zhu, M. Janoschek, D. S. Chaves *et al.*, "Electronic correlation and magnetism in the ferromagnetic metal Fe_3GeTe_2," Phys. Rev. B **93**, 144404 (2016).

[34]F. Huang, G. J. Mankey, M. T. Kief, and R. F. Willis, "Finite-size scaling behavior of ferromagnetic thin films," J. Appl. Phys. **73**, 6760 (1993).

[35]R. Skomski and J. M. D. Coey, "Magnetic anisotropy—How much is enough for a permanent magnet?," Scr. Mater. **112**, 3 (2016).

[36]Z. S. Lin, M. Lohmann, Z. A. Ali *et al.*, "Pressure-induced spin reorientation transition in layered ferromagnetic insulator $Cr_2Ge_2Te_6$," Phys. Rev. Mater. **2**, 051004(R) (2018).